A study of macrophysical and microphysical properties of warm clouds over the Northern Hemisphere using CloudSat/CALIPSO data

Wenhua Gao[1], Chung-Hsiung Sui[2], and Zhijin Hu[3]

[1]State Key Laboratory of Severe Weather, Chinese Academy of Meteorological Sciences, Beijing

[2]Department of Atmospheric Sciences, National Taiwan University, Taipei

[3]Weather Modification Center of China Meteorological Administration, Chinese Academy of Meteorological Sciences, Beijing

Abstract

This study investigates the general macrophysical and microphysical properties of single-layer warm clouds over the Northern Hemisphere (NH) ocean and land areas using four standard CloudSat products during the period of 2008. The yearly averaged occurrence frequency of single-layer warm clouds is 20.9% oceans and 9.5% land, and the total hydrometeor covers 77.5% and 65.8%, respectively. The cloud base heights (CBHs) of single-layer warm clouds are approximately 1 km, and the geometrical thicknesses over land are 0.5-1 km thicker than those over oceans. Results show that the maximum values of liquid water content (LWC) over land are about 10-30% smaller and the occurring altitudes are nearly 0.5 km higher as compared to those over oceans with the same liquid water path (LWP), which is likely related to the weak upward motions and large surface evaporation over oceans. Moreover, the microphysical properties are analyzed to examine the growth processes of cloud particles from cloud to drizzle and to rain within warm clouds and how these processes vary with increasing LWP. When LWP is less than 0.5 mm, cloud droplets at the base of clouds grow primarily by condensation process. With increasing LWP up to 1.0 mm, radar reflectivity gradually increases from cloud top downward, indicating a growth of drizzle drops by collection of small droplets. As LWP becomes

larger than 1.0 mm, raindrops begin to form and develop sufficiently. Note that the evolutions of contoured frequency by altitude diagrams (CFADs) of radar reflectivity over land always appear later and dBZ values are a little smaller than those over oceans with the same LWP. It is probably due to the influence of continental aerosol in this area, suggesting that high aerosol concentrations may induce a suppressed drizzle and delayed precipitation process in warm clouds. However, the cloud particle size at the upper part of clouds over land is somewhat larger than that over oceans. This is inconsistent with our general understanding about the aerosol effect on droplet size. It should be attributed to a stronger vertical air motion over land, which transports large particles to the upper part of clouds. In addition, the shape of particle size spectrum is produced by a balance between breakup and coalescence processes when LWP is greater than 2.0 mm. The results of this study provide valuable references for cloud-resolving models simulations.

We highlight the key finding that there exists a significant difference between ocean and land areas in the period of warm clouds formation in contoured frequency by optical depth diagrams (CFODDs) of radar reflectivity. When LWP is 0.1-0.2 mm and optical depth exceeds 25, the dBZ values over oceans increase rapidly downward with increasing optical depth (decreasing height). The faster growth of particles may be caused by the evaporation-condensation mechanism, which can occur under a certain water vapor environment. However, large droplets are unlikely to appear in the early stage of continental warm clouds because of the aerosol effect, preventing the evaporation-condensation mechanism to occur, and resulting in partially delayed drizzle formation over land.

Keywords: warm clouds, macrophysical and microphysical properties, Northern Hemisphere, CloudSat

1. Introduction

Clouds and associated thermodynamic processes are crucial components of the Earth's climate system because of their profound influences on hydrologic cycle and planetary radiation budget. Various clouds types (e.g., altitude, hydrometeor phase, and optical thickness, etc.) have different effects on incoming shortwave and outgoing longwave fluxes [Hartmann et al., 1992; Stephens, 2005]. The occurrence of low clouds over the Southern Hemisphere oceans is high, with 79% of all cloud layers observed having tops below 3 km [Haynes et al., 2011]. In addition, rain from single-layer warm clouds over the global oceans comprised 31.2% (35.3%) of rain occurrences and 17.0% (19.2%) of total rain volume for January (July) 2008 [Chen et al., 2011]. Therefore, investigation of the general macrophysical and microphysical properties of clouds, especially the low warm clouds, is fundamental importance to improve our understanding on the life cycle of these clouds and their effects on energy and water balances of the climate system.

The satellite-based measurements are highly effective and convenient methods to explore global cloud systems. However, passive satellite sensors can only observe cloud properties of integrated paths or near cloud tops. We know that the vertical distributions and internal structures of cloud optical properties can be used to provide more insights into microphysical properties indicative of microphysical processes during different stages of cloud life cycles. Recently, vertical cloud structures have begun to be observed globally by satellite-borne active sensors (e.g., the W-band Cloud Profiling Radar [CPR, Im et al., 2005] and Cloud-Aerosol Lidar with Orthogonal Polarization [CALIOP, Winker et al., 2003]). They both flied as part of the A-Train satellite constellation [Stephens et al., 2002], along with the Moderate Resolution Imaging Spectroradiometer (MODIS) on board the Aqua satellite. The CPR, on board CloudSat, is sensitive to cloud and weak precipitation particles and has offered unique global coverage of cloud vertical structure at high vertical resolution [Stephens et al., 2008]. The CALIOP on board Cloud-Aerosol Lidar and Infrared Pathfinder Satellite Observations (CALIPSO) is sensitive to optically thin clouds that

could be missed by CPR. So, combined CloudSat and CALIPSO observations have provided new opportunities for quantitative estimations of cloud microphysics and rainfall parameters in precipitating cloud systems where signal attenuations are not very severe [Stephens et al., 2002; Matrosov, 2007, 2008]. The combined data also provide more in-depth global measurements for determining statistical characteristics of cloud vertical structure.

A few recent studies have demonstrated the values of CloudSat and CALIPSO in combination with other measurements, to investigate the clouds macrophysics and microphysics, especially for warm liquid clouds. Luo et al. [2009] showed that the averaged hydrometeor occurrence frequency is 80% for eastern China and 70% for Indian region, to which single-layer hydrometeors contribute 63% and 53% by using CloudSat standard products during the period July 2006 to August 2007. Kubar et al. [2009] indicated the importance of macrophysical variables (e.g., cloud thickness, liquid water path (LWP)) and microphysical variables (e.g., effective radius, number concentration) on warm drizzle intensity and frequency across the tropics and subtropics using CloudSat cloud radar and MODIS optical data. Nakajima et al. [2010] inferred the droplet growth process from cloud to rain via drizzle proceeds monotonically with the evolution of particle radius in warm water clouds by A-Train observations. Suzuki et al. [2010] combined CloudSat and MODIS data to study the microphysical processes of warm clouds on the global scale, and found a multimodal distribution in satellite-observed reflectivity profiles and interpreted them in terms of drop collection processes based on the continuous collection model. These results provide a quantitative description about insight into the characteristics of warm clouds in real atmosphere.

Because of the complexity of multi-layer clouds, in this paper, we focus on single-layer warm clouds in the Northern Hemisphere (NH). The warm clouds have relatively straightforward microphysical processes but result in significant precipitation. Cloud microphysical properties are crucial for understanding the evolution processes between different forms of hydrometeors and final surface precipitation. We here explore the internal structures of warm clouds and related

microphysical processes by analyzing statistics of large numbers of CPR reflectivity in the entire NH. More specifically, occurrence frequency, cloud base height (CBH), cloud top height (CTH), liquid water content (LWC), and radar reflectivity distribution of single-layer warm clouds during 2008 are analyzed. We attempt to demonstrate the differences in the growth process of cloud particles in various stages of evolution between the ocean and land areas and reveal the reasons for the differences.

The major objective of this paper is to advance the understanding of general macrophysical and microphysical properties of single-layer warm clouds as well as the microphysical evolution mechanism of warm clouds precipitation using CloudSat observations. These results provide us a valuable reference for evaluating outputs from cloud-resolving models. The data and method are described in sections 2. Analyses results are presented in sections 3, including occurrences of cloud layers, CBH and CTH, and in section 4 including LWC, radar reflectivity, and liquid effective radius. Section 5 contains the conclusions and summary.

2. Data and method

We utilize the latest version of CloudSat standard data products, 2B-GEOPROF, 2B-CLDCLASS-LIDAR, 2B-CWC-RVOD, and 2B-TAU for the year of 2008 in the present study. Specifically, vertical distributions of radar reflectivity are from 2B-GEOPROF [Marchand et al., 2008], liquid water content and liquid effective radius are from 2B-CWC-RVOD [Wood, 2008], number of layers, cloud phase, cloud top and cloud base heights are from 2B-CLDCLASS-LIDAR [Wang et al., 2013], and profiles of optical depth are from 2B-TAU [Polonsky et al., 2008], respectively. 2B-CLDCLASS-LIDAR combines CloudSat CPR and CALIPSO lidar cloud masks. 2B-CWC-RVOD and 2B-TAU contain MODIS visible optical depth analysis interpolated in time and space to the CloudSat track. A forward model is employed in the retrieval algorithm to estimate the number concentration, radius, and width parameter required to compute LWC. By an optimal estimation technique, the forward

model relates a state vector of known quantities (radar reflectivity and visible optical depth) to a state vector of unknowns (number concentration, radius, and width parameter). The priori values of unknowns are assigned based on the climatological values of relevant variables.

Due to the surface return contamination, hydrometeors in the first kilometer above the surface cannot be detected well with CloudSat [Marchand et al., 2008], so the data from the lowest 1km should be used carefully. In this study, a total of 3698 tracks (including the above four product files) are available over the NH in an entire year of 2008. All the data are at the spatial grid of the CPR with resolutions of 2.5 km along track by 1.4 km across track and 240 m in the vertical. Moreover, to obtain high quality cloud information, a confidence quality flag of great 5 for cloud phase and an unconfidence quality flag of less 50 for LWC from the corresponding product files are used to select the cloud profiles, and all the statistical analyses except the occurrence frequency of hydrometeor are performed with column optical depth greater than 0.1.

The contoured frequency by altitude diagrams [CFADs, Yuter and Houze, 1995] are constructed where radar reflectivity is larger than the minimum detectable signal [-30 dBZ, Tanelli et al., 2008] to gain the vertical distributions of hydrometeors and possible microphysical processes within clouds. The optical depth at height h from the cloud top that used in section 4.2d is inferred from the 2B-TAU data by integrating the layer optical depth above h. The analyses are restricted to single-layer and warm liquid clouds only. The former is determined as the number of cloud layers is 1 by radar-lidar combined measurements, and the latter is identified as the cloud phase is water in the 2B-CLDCLASS-LIDAR product derived from CALIPSO features, temperature, and radar reflectivity. Furthermore, to study the temporal changes in warm clouds structures, the cloud LWP, generally controlled by both cloud-scale dynamics and thermodynamics of ambient air [Petty, 2006], is employed to serve as an indirect indicator for the life stages of warm clouds. Chen et al. [2011] suggested that the cloud LWP is the best potential for detecting warm rain events and estimating the rain rates. We form the ensemble averages of different variables as a function of LWP values in the following five groups 0-0.5, 0.5-1.0, 1.0-1.5, 1.5-2.0, and 2.0-2.5

mm, respectively.

3. Macrophysical properties

We first discuss macrophysical cloud properties that satellite instruments are particularly well-suited to observing, such as the occurrence frequency, cloud height, and geometrical depth of a warm cloud.

3.1. Occurrence frequencies of single- and multilayer clouds

In this study, a profile is identified as cloudy when there is at least one hydrometeor layer in the column. The area-averaged occurrence frequencies of single-, double-, and multilayer clouds are determined as the number of profiles containing single-, double-, and multilayer clouds divided by the total number of profiles collected in the given area, respectively. The total occurrence frequencies are the sum of frequencies of all layer types. There are 40301330 and 27955547 profiles over the NH ocean and land areas, respectively, in the year of 2008. Among them, 77.5% and 65.8% are cloudy profiles. That is, the total cloud cover over land is approximately 10 percent lower than those over oceans. The occurrences of single-layer clouds are the highest, which contribute 47.1% and 40.8% to the total profiles observed. The occurrences of double-layer clouds account for about one-fifth of the total profiles. The single-layer warm clouds we concerned about here also occur relatively frequently, which contribute 20.9% over oceans, 9.5% over land, respectively, and only slightly smaller than that of double-layer clouds over the ocean (Table 1).

Figure 1 shows the monthly variations of occurrence frequencies of total, single-, double-, and multilayer clouds over the NH. The total occurrences of hydrometeor are between 0.7 and 0.8 over oceans, between 0.6 and 0.7 over land, and are relatively constant among the seasons in such a large area. Similar results were obtained by Wylie et al. [2005] over the 20°N-60°N latitude using 22-yr High Resolution Infrared Radiometer Sounder (HIRS) satellite data. The monthly occurrences of single-, double-, and multilayer clouds also remain near unchanged through the year only with those over oceans change slightly higher. Note that the trends of double-layer clouds

are roughly similar to those of the total occurrences, indicating that the monthly variations in the double-layer clouds partially cause the pronounced changes with season in the total occurrences. The relatively high occurrences of double- and multilayer clouds during May to October suggest more complicated cloud-layer structures associated with the summer monsoon and large scale circulation over the NH. As for the single-layer warm clouds, which are strongly correlated with the atmospheric temperature, vary significantly with season with maxima during the summer months and minima during winter months. The single-layer warm clouds account for a considerable fraction of the total occurrence frequencies, especially in the summer months.

3.2. PDFs of base and top heights

The probability distribution functions (PDFs) of cloud base and cloud top heights of single-layer warm clouds are shown in Figure 2. It is remarkable that the CBHs have one dominant mode of near 1 km over the ocean. Due to the reflection from the surface and the 1 km pulse length of CPR, sensitivities of the CPR in the lowest 1 km near the surface are reduced [Li et al., 2013]. The uniform lower boundary might be a consequence of the limitation in CloudSat observations. With regard to the upper boundary for these liquid phase clouds, there is no evidence of any immediate bias in the CloudSat algorithm. The CTHs of maximum occurrence frequency shift toward higher values (from 1.5 to 3.5 km) over oceans as LWP increases. i.e., the cloud geometrical thickness increases with the cloud system development. Figs.2c and 2d show analogous PDFs but over land. One apparent difference between them is that the CTHs distributions tend to be less centralized, especially at larger LWPs, and a large number of warm clouds have CTHs that surpass 5 km when LWP is great than 1.0 mm. It indicates that the warm cloud systems over land are geometrically thicker than those over oceans and suggests that convection over land grows stronger and deeper than oceanic convection does. Catto et al. [2012] also demonstrated that precipitation over the NH continents is mainly associated with warm fronts. These notions are discussed more in depth in the coming sections. Additionally, increasing cloud top

height along with cloud LWP indicates that these two macrophysical quantities are quite related to each other [Kubar et al., 2009]. Clouds grow vertically and thus contain more liquid water when more drizzle produced.

4. **Microphysical properties**

While the microphysical properties of clouds are predominantly measured by in-situ and aircraft-mounted instruments, the combinations of new-generation active satellite-borne sensors enable indirect estimates of internal microphysical properties in warm clouds.

4.1. Profiles of LWC

Liquid water content is a key characteristic tightly linked to microphysical and dynamical processes of clouds, and remains to be one of the major sources of model differences [Li et al., 2008]. Figure 3 shows the vertical profiles of cloud LWC with various LWP. The average LWC at height h is calculated only when cloud is present at this height. Over oceans, the peak values of LWC shift toward higher values as LWP increases. i.e., the magnitudes of LWC gradually increase with the evolution of warm cloud systems. Meanwhile, the height of maximum LWC also steadily increases from 1.0 km to about 2.5 km as LWP changes from (0.5-1.0 mm) to (2.0-2.5mm). In contrast, the vertical characteristics over land are somewhat different from those over oceans. The maximum values of LWC are 10-30% smaller during the same stage of cloud development (i.e. the same LWP) and the occurring heights are about 0.5 km higher over land. The reason for these differences should be the weaker upward motions as well as larger surface evaporation over oceans. Note that the magnitudes of LWC quickly drop to zero below 0.7 km where the CloudSat algorithm cannot assign the radar return. The values below 1 km should be viewed with caution.

4.2. CFADs of radar reflectivity

The CFAD diagrams shown in Figure 4 are formed by contouring the frequency of radar reflectivity (in 1dB bins) as a function of altitude (in 0.24 km bins) for all cloudy profiles. The radar reflectivity in the ranges of less than -20, -15 to 0, and 0 to

10 dBZ, are respectively interpreted as corresponding to cloud, drizzle, and rain [Suzuki et al., 2010]. When LWP is less than 0.5 mm (Fig. 4a), the highest occurrence frequency of reflectivity is almost all smaller than -20 dBZ through the entire cloud layers, indicating the clouds are mainly consisted of small droplets. The feature of upward particle growth below 1.5 km is due to the condensation process driven by uplifting air until the small cloud droplets become embryos of drizzle. In contrast, the reflectivity above 1.5 km tends to decrease gradually with increasing height, likely due to the evaporation process induced by entrainment that often occurs in the vicinity of cloud top. Meanwhile, low level clouds have reflectivity values covering a wide range, indicating that the radii of cloud droplets begin to vary significantly and evolve gradually to drizzle mode. With increasing LWP up to 1.0 mm (Fig. 4b), the occurrence around -15 to 0 dBZ becomes pronounced (drizzle mode). The tendency of reflectivity monotonically increases from cloud top with decreasing height, reflecting downward growth of drizzle particles by aggregation or accretion of cloud droplets in the lower part of cloud layers. When LWP is up to 1.5 mm, the radar reflectivity continues to grow downward and reaches a value of 5 dBZ near 1.5 km height as shown in Fig. 4c. This feature represents the raindrops begin to form and the drizzle mode has slowly transitioned into rain mode. In Figs. 4d and 4e, the frequencies of reflectivity around 0-10 dBZ tend to become more pronounced and eventually reach 10 dBZ in the middle part of cloud layers, illustrating how the rain mode becomes dominant when LWP is greater than 1.5 mm. Note that the values of reflectivity increase rapidly from 0 to 10 dBZ above 1.5 km, while decrease gradually to near 0 dBZ below 1.5 km as shown in Fig. 4e. This is likely due to the strong signal attenuation by large hydrometeors above 1.5 km and the raindrop evaporation when falling out of cloud base in lower troposphere. Note that the occurring locations of the highest frequency are corresponding to the altitude of maximum LWC layer shown in Fig. 3, reflecting the collection growth process of raindrops with liquid cloud water at different heights. Overall, these characteristics in Figs. 4a-4e clearly demonstrate the growth processes of cloud droplets to drizzle drops and to rain drops with increasing LWP.

Figures4f-4j show the similar transition processes from cloud to rain but over land. Two significant differences are found between the ocean and land areas. One is the evolutionary processes of radar reflectivity over land always appear later and the dBZ values of maximum occurrence frequency are always smaller but occurring locations are higher than those over oceans with the same LWP. The evolution delay and smaller reflectivity (i.e., smaller radius) are probably due to the influence of continental aerosol in land area. This confirms that high aerosol concentration may suppress drizzle formation and delay precipitation process as reported in previous studies [Albrecht, 1989; Rosenfeld, 1999, 2000; Li et al., 2011]. Another significant difference is the smaller variation in the vertical between 3 and 1 km (i.e., extending deeper) over land after the rain formation, especially when LWP is more than 2.0 mm, which should attribute to the stronger vertical motions to advect large particles upward. Due to the upward air motions, the particle spectral shapes are then produced by a balance between breakup and coalescence processes. In addition, the tops of 1% contour (outermost contour) of radar reflectivity over oceans increase steadily with increasing LWP; however, those over land generally reach a higher altitude (i.e., higher cloud tops), further revealing that convection is relatively deeper and stronger over the land area (likely as a result of uneven surface heating). In contrast, oceanic clouds are more prone to develop stratiform precipitation because of the warm moist boundary layer and near-moist adiabatic stratification of the free atmosphere [Schumacher and Houze, 2003].

4.3. CFADs of liquid effective radius

Figure 5 shows the CFADs of liquid effective radius. At the first glance, one might readily find that the effective radii increase gradually from nondrizzling cloud to drizzle and rain in the lower part of clouds. It appears that the microphysical changes are more evident at the onset of drizzle (Fig. 5b). Drizzle has the significant effect on scavenging cloud condensation nuclei (CCN), and lower CCN concentration is favorable to the formation of drizzle, suggesting a positive feedback [Wood, 2006]. The average particle size increases rapidly downward from 4 to 2 km height with

maximum value reached near 2 km (Figs. 5c-5e). This indicates that the hydrometeor particles grow larger as they fall, and cumulate around at 2 km due to dynamical and microphysical processes. The most important is that the particle radius tends to be somewhat smaller below 3 km over land compared to that over oceans during the rain formation stage. The smaller particle size over land is due to the influence of continental aerosol (commonly surpassing 300 cm^{-3}). This is consistent with the results of previous studies. However, the particle size above 3 km over land is obviously larger than that over oceans when LWP is great than 1.0 mm. This seems inconsistent with our general understanding on the aerosol indirect effect as a reduction in droplet size, which is mainly attributed to the stronger vertical air motions that transport large particles to the upper part of clouds.

4.4. CFODDs of radar reflectivity

Nakajima et al. [2010] proposed a contoured frequency by optical depth diagrams (CFODDs), in which the reflectivity profiles are rescaled as a function of the in-cloud optical depth. The slope of reflectivity varying with optical depth implies the drop collection process and provides a gross indicator for the collection efficiency factor. Figure 6 shows the CFODDs of radar reflectivity grouped according to LWP with an interval of 0.1 mm in order to pay more attention to the early development stages of warm clouds formation. The slopes of the upper part (optical depth <10) of reflectivity profiles gradually become steeper with increasing LWP, implying the increasing collection efficiencies during the evolution of warm clouds. The key finding here is that there exists a significant difference between ocean and land areas when LWP is between 0.1 and 0.2 mm and optical depth exceeds 25 as shown in Figs. 6b and 6g. Under these conditions, radar reflectivities over oceans increase rapidly downward with increasing optical depth (decreasing height) and reach a value of -10 dBZ, indicating that the drizzle drops begin to form. On the other hand, a significant portion of reflectivities over land are still smaller than -20 dBZ. Since the particle size (i.e., collection efficiency) is still very small at this early stage of cloud formation, we speculate that the growth of cloud particles is possibly resulted from the

evaporation-condensation mechanism. The large drops are saturated but the small droplets are unsaturated in certain water vapor conditions because of the droplet curvature effect. As a result, the large drops can grow through condensation at the expense of small droplets that evaporate, and rapidly convert to drizzle drops. However, few large drops exist over land in the early stage of warm clouds formation in the presence of continental aerosols, and the evaporation-condensation mechanism hardly occurs, partially resulting in a delayed drizzle formation over the land area.

5. Conclusions and summary

The general macrophysical properties (hydrometeor occurrence frequency, cloud base and cloud top heights) and microphysical properties (liquid water content, effective radius, and radar reflectivity) of single-layer warm clouds over the Northern Hemisphere ocean and land areas are investigated using four latest standard CloudSat products: GEOPROF, CWC-RVOD, CLDCLASS-LIDAR, and TAU during the period of 2008. The yearly averaged total occurrence frequency of hydrometeor is 77.5% over oceans and 65.8% over land, and the single-layer warm clouds contribute 20.9% and 9.5%, respectively. The single-layer warm clouds vary significantly with season with maxima during summer months and minima during winter months.

The LWP is employed in this study to serve as an indicator for the life stages of clouds. The CBHs of single-layer warm clouds remain near 1 km without much change for different development stages of cloud systems; however, the CTHs continuously move up as LWP increases. The geometrical thicknesses of single-layer warm clouds over land are approximately 0.5-1 km thicker than those over oceans. Results show that the magnitudes of LWC gradually increase with the evolution of warm clouds, and the occurring altitudes of maximum LWC also steadily rise. The maximum values of LWC over land are generally 10-30% smaller and the occurring heights are about 0.5 km higher compared to those over oceans with the same LWP. The differences are more likely caused by the weaker upward motions but larger surface evaporation over oceans than over land.

The CFADs of radar reflectivity and their change with increasing LWP clearly illustrate the growth processes from cloud droplets to drizzle and then to rain drops within the warm cloud layers. When LWP is less than 0.5 mm, the cloud droplets dominate the whole cloud layers and only grow via condensation process. When LWP becomes larger than 0.5 mm, the tendency of reflectivity increases from cloud top downward, indicating the appearance of drizzle as a consequence of more prevalent aggregation and accretion of cloud droplets. At the following development stages (when LWP becomes larger than 1.0 mm), rain begin to show a sustainable development. Note that the evolutions of radar reflectivity over land always appear later and reflectivity values are generally smaller than those over oceans at the same LWP. The evolution delay along with the small dBZ is probably due to the influence of continental aerosol. The high aerosol concentration can induce suppressed drizzle and delayed precipitation process in warm clouds. In addition, the reflectivity values over land are almost constant with height when LWP is great than 2.0 mm, which is likely a result of balance between breakup and coalescence processes in the presence of stronger updrafts. Moreover, the cloud particle size at the upper part of clouds over land is somewhat larger than that over oceans when LWP is great than 1.0 mm, and it is inconsistent with our basic understanding of the aerosol effect on particle size. This is caused by the stronger vertical air motion over land that transports large particles to the upper part of clouds.

We also found that there exists a significant difference in CFODDs of radar reflectivity between the ocean and land areas when LWP is 0.1-0.2 mm and optical depth exceeds 25. The faster growth of particles over oceans under these conditions is possible due to the evaporation-condensation mechanism, which can occur in a certain water vapor environment. However, few large drops exist in the early stage of warm clouds in the presence of aerosols over land, so the evaporation-condensation mechanism is less likely to occur, resulting in partially delayed drizzle formation over land.

Acknowledgments. The authors are grateful to the anonymous reviewers for their valuable comments on an earlier version of this paper. W. Gao was supported by the National Program on Key Basic Research Project of China (Grant No. 2013CB955804, 2011CB403401). C.-H. Sui was supported by the National Science Council NSC_98-2745-M-002-011-ASP. The CloudSat data were provided by the CloudSat Data Processing Center at http://www.cloudsat.cira.colostate.edu.

References

Albrecht, B. A. (1989), Aerosols, cloud microphysics, and fractional cloudiness, *Science*, 245, 1227-1230.

Catto, J. L., C. Jakob, G. Berry, and N. Nicholls (2012), Relating global precipitation to atmospheric fronts, *Geophys. Res. Lett.*, 39, L10805, doi:10.1029/2012GL051736.

Chen, R., Z. Li, R. J. Kuligowski, R. Ferraro, and F. Weng (2011), A study of warm rain detection using A-Train satellite data, *Geophys. Res. Lett.*, 38, L04804, doi:10.1029/2010GL046217.

Hartmann, D. L., M. E. Ockert-Bell, and M. L. Michelsen (1992), The effect of cloud type on Earth's energy balance: Global analysis, *J. Climate*, 5, 1281-1304.

Haynes, J. M., C. Jacob, W. B. Rossow, G. Tselioudis, and J. Brown (2011), Major characteristics of Southern Ocean cloud regimes and their effects on the energy budget, *J. Climate*, 24, 5061-5080.

Im, E., C. L. Wu, and S. L. Durden (2005), Cloud profiling radar for the CloudSat mission, *IEEE Aerosp. Electron. Syst. Mag.*, 20, 15-18.

Kubar, T. L., D. L. Hartmann, and R. Wood (2009), Understanding the importance of microphysics and macrophysics for warm rain in marine low clouds. Part I: Satellite observations, *J. Atmos. Sci.*, 66, 2953-2972, doi: 10.1175/2009JAS3071.1.

Li, J.-L. F., et al. (2008), Comparisons of satellites liquid water estimates to ECMWF and GMAO analyses, 20th century IPCC AR4 climate simulations, and GCM simulations, *Geophys. Res. Lett.*, 35, L19710, doi:10.1029/2008GL035427.

Li, J. M., Y. H. Yi, K. Stamnes, X. D. Ding, T. H. Wang, H. C. Jin, and S. S. Wang (2013), A new approach to retrieve cloud base height of marine boundary layer clouds, *Geophys. Res. Lett.*, 40, 4448-4453, doi:10.1002/grl.50836.

Li, Z., F. Niu, J. Fan, Y. Liu, D. Rosenfeld, and Y. Ding (2011), The long-term impacts of aerosols on the vertical development of clouds and precipitation, *Nature Geoscience*, 4, 888-894, doi:10.1038/ngeo1313.

Luo, Y., R. Zhang, and H. Wang (2009), Comparing occurrences and vertical structures of hydrometeors between the eastern China and the Indian monsoon region using *CloudSat*/CALIPSO data, *J. Clim.*, 22, 1052-1064.

Matrosov, S. Y. (2007), Potential for attenuation-based estimations of rainfall rate from CloudSat, *Geophys. Res. Lett.*, 34**,** L05817, doi:10.1029/2006GL029161.

Matrosov, S. Y. (2008), Assessment of radar signal attenuation caused by the melting hydrometeor layer, *IEEE Trans. Geosci. Remote Sens.*, 46**,** 1039-1047.

Marchand, R., G. G. Mace, T. Ackerman, and G. Stephens (2008), Hydrometeor detection using CloudSat-An earth-orbiting 94-GHz cloud radar, *J. Atmos. Oceanic Technol.*, 25, 519-533.

Nakajima, T. Y., K. Suzuki, and G. L. Stephens (2010), Droplet growth in warm water clouds observed by the A-Train. Part II: A multisensory view, *J. Atmos. Sci.*, 67, 1897-1907.

Petty, G. W. (2006), *A first course in atmospheric radiation*, 2nd ed. Sundog Pub., Wisconsin, 452 pp.

Polonsky, I., et al. (2008), CloudSat Project: *Level 2 cloud optical depth product process description and interface control document*, Colorado State University, Colorado, 21pp.

Randall, D. A., J. A. Coakley Jr., C. W. Fairall, R. A. Kropfli, and D. H. Lenschow (1984), Outlook for research on subtropical marine stratiform clouds, *Bull. Amer. Meteor. Soc.*, 65, 1290-1301.

Rosenfeld, D. (1999), TRMM observed first direct evidence of smoke from forest fires inhibiting rainfall, *Geophys. Res. Lett.*, 26, 3105-3108.

Rosenfeld, D. (2000), Suppression of rain and snow by urban and industrial pollution, *Science*, 287, 1793-1796.

Schumacher, C., and R. A. Houze (2003), Stratiform rain in the tropics as seen by the TRMM precipitation radar, *J. Climate*, 16, 1739-1756.

Stephens, G. L., et al. (2002), The CloudSat mission and the A-train. A new dimension of space-based observations of clouds and precipitation, *Bull. Amer. Meteor. Soc.*, 83**,** 1771-1790.

Stephens, G. L. (2005), Cloud feedbacks in the climate system: A critical review, *J. Climate*, 18,

237-273.

Stephens, G. L., et al. (2008), The CloudSat mission: Performance and early science after the first year of operation, *J. Geophys. Res.*, 113, D00A18, doi:10.1029/2008JD009982.

Suzuki, K., T. Y. Nakajima, and G. L. Stephens (2010), Particle growth and drop collection efficiency of warm clouds as inferred from joint CloudSat and MODIS observations, *J. Atmos. Sci.*, 67, 3019-3032.

Tanelli, S., S. L. Durden, E. Im, K. S. Pak, D. G. Reinke, P. Partain, J. M. Haynes, and R. T. Marchand (2008), Cloudsat's cloud profiling radar after 2 years in orbit: Performance, external calibration, and processing, *IEEE Trans. Geosci. Remote Sens.*, 46, 3560-3573.

Wang, Z., et al. (2013), CloudSat Project: *Level 2 combined radar and lidar cloud scenario classification product process description and interface control document*, California Institute of Technology, California, 61pp.

Winker, D. M., J. R. Pelon, and M. P. McCormick (2003), The CALIPSO mission: Spaceborne lidar for observation of aerosols and clouds, *Proc. SPIE* 4893, Lidar Remote Sensing for Industry and Environment Monitoring III, doi:10.1117/12.466539.

Wood, N. (2008), CloudSat Project: *Level 2B radar-visible optical depth cloud water content (2B-CWC-RVOD) process description document*, Colorado State University, Colorado, 26pp.

Wood, R. (2006), Rate of loss of cloud droplets by coalescence in warm clouds, *J. Geophys. Res.*, 111, D21205, doi:10.1029/2006JD007553.

Wylie, D. P., D. L. Jackson, W. P. Menzel, and J. J. Bates (2005), Trends in global cloud cover in two decades of HIRS observations, *J. Climate*, 18, 3021-3031.

Yuter, S. E., and R. A. Houze (1995), Three-dimensional kinematic and microphysical evolution of Florida cumulonimbus. Part II: Frequency distributions of vertical velocity, reflectivity, and differential reflectivity, *Mon. Wea. Rev.*, 123, 1941-1963.

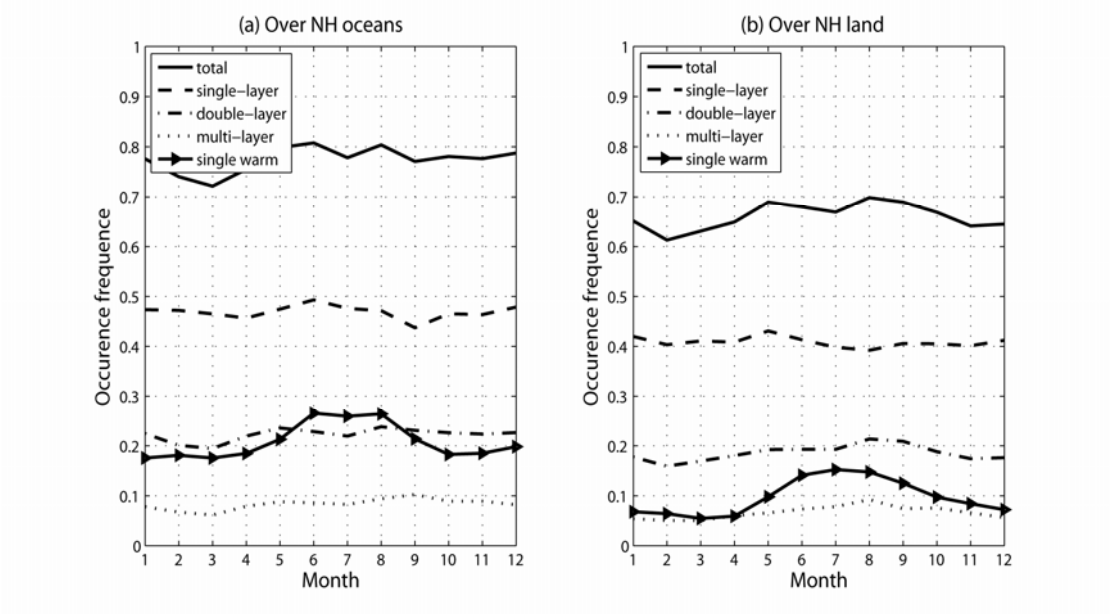

Figure 1. Monthly averaged occurrence frequencies of all cloud layers and single-, double-, and multilayer clouds, respectively, over (a) NH oceans and (b) NH land during 2008.

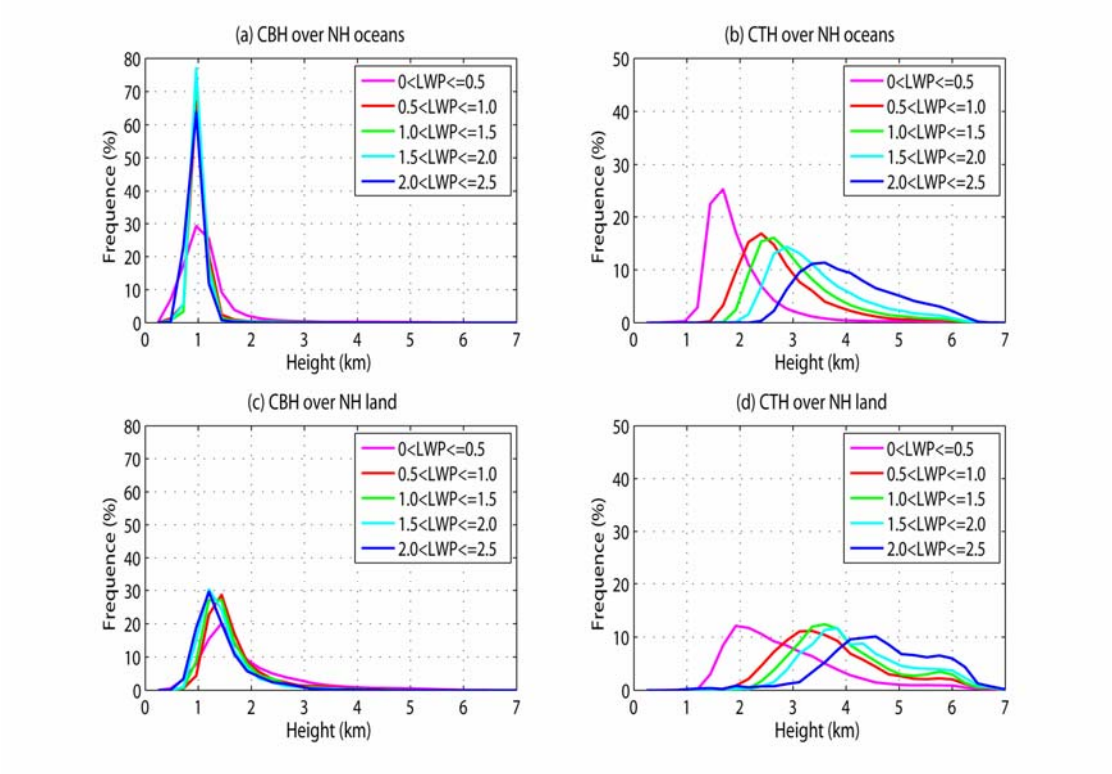

Figure 2. PDFs of (left) cloud base heights and (right) cloud top heights for single-layer warm clouds over (top) NH oceans and (bottom) NH land. Color solid lines denote the various LWP with an interval of 0.5 mm.

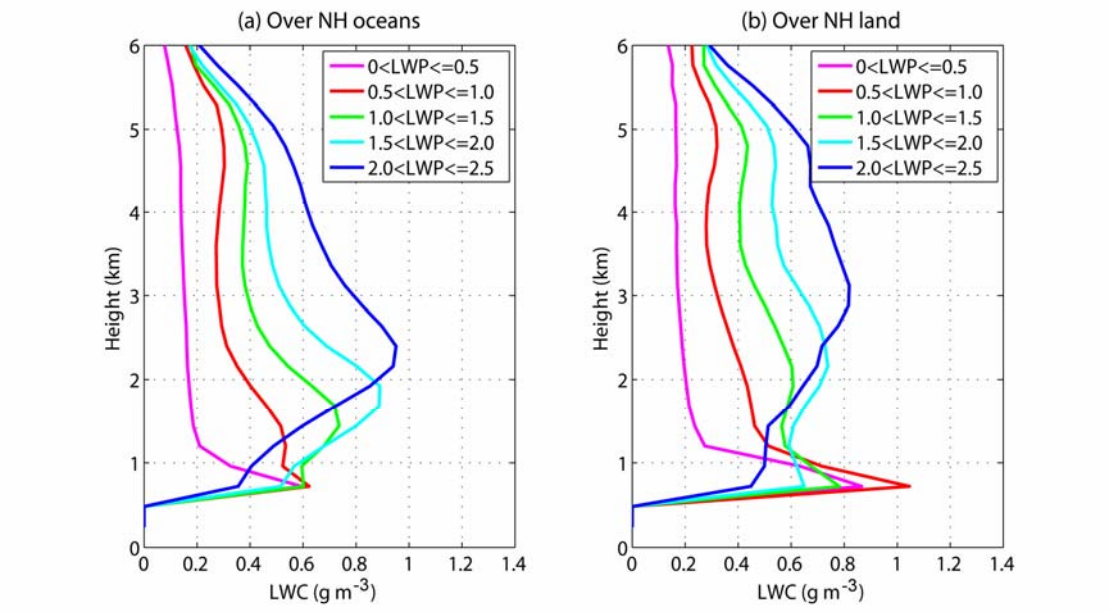

Figure 3. Vertical profiles of LWC over (a) NH oceans and (b) NH land. Color solid lines denote the various LWP with an interval of 0.5 mm.

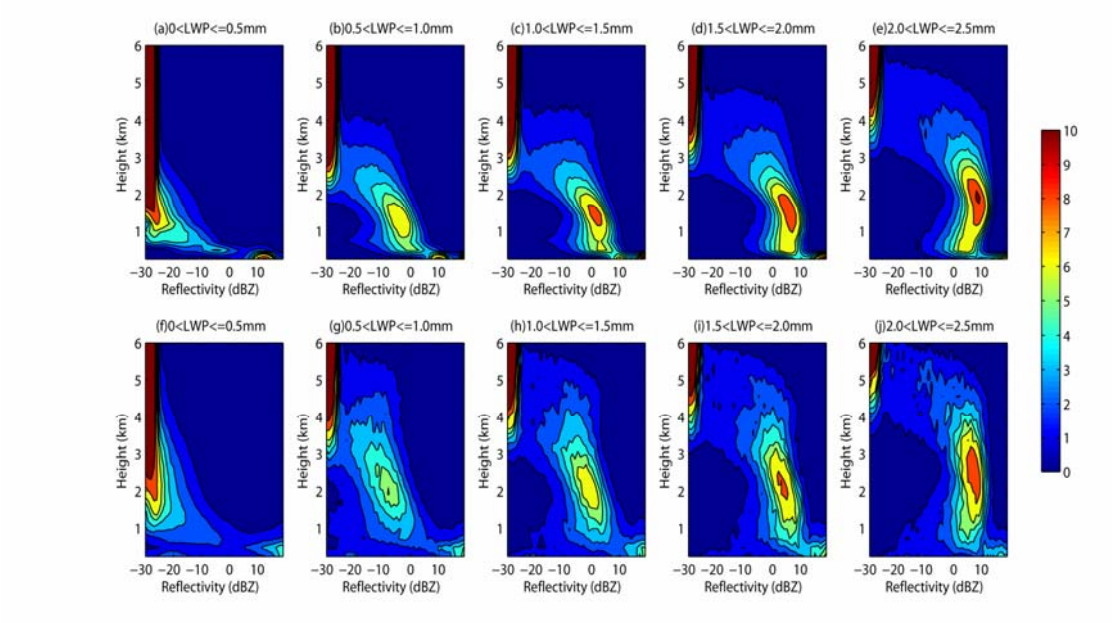

Figure 4. CFADs of radar reflectivity for all cloudy profiles grouped according to LWP with an interval of 0.5 mm over (top) NH oceans and (bottom) NH land. The bin size is 1 dBZ in the horizontal and 0.24 km in the vertical.

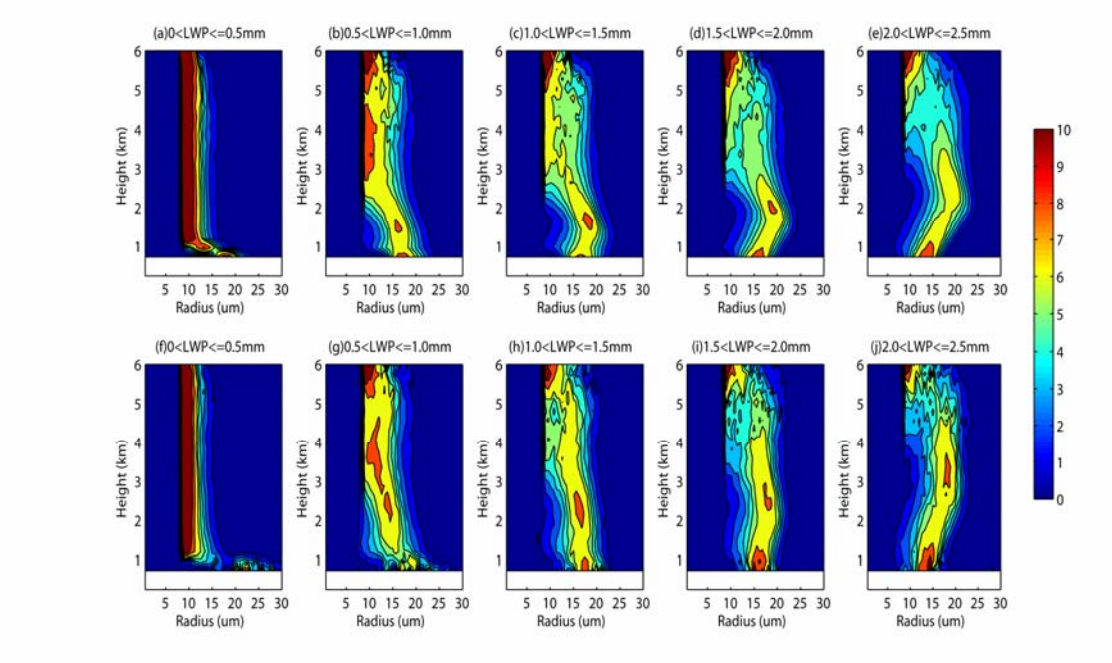

Figure 5. Same as Fig. 4, but for liquid effective radius.

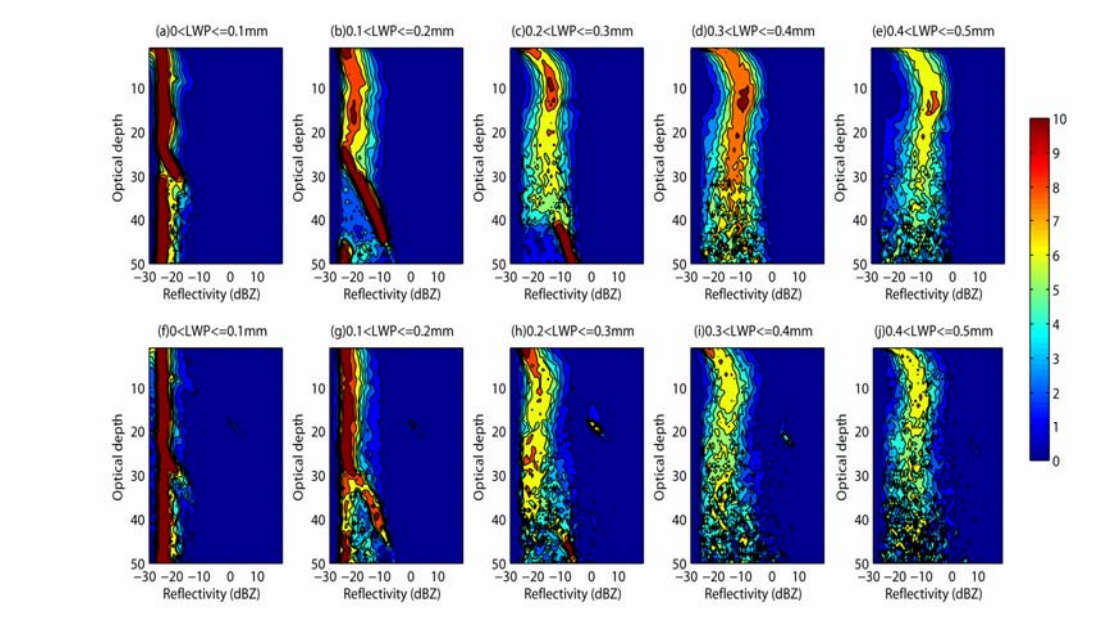

Figure 6. CFODDs of radar reflectivity for all cloudy profiles grouped according to LWP with an interval of 0.1 mm over (top) NH oceans and (bottom) NH land. The bin size is 1 dBZ in the horizontal and 1 (optical depth) in the vertical.

Table 1. The numbers of all profiles, fractions of cloudy profiles and single-, double-, multilayer clouds, respectively, over NH oceans and NH land during 2008.

	All	Cloudy	Single-layer	Double-layer	Multi-layer	Single-layer warm
land	27955547	65.8%	40.8%	18.4%	6.6%	9.5%
ocean	40301330	77.5%	47.1%	22.2%	8.2%	20.9%